GENETICS

Supporting Information
http://www.genetics.org/cgi/content/full/genetics.109.108688/DC1

Interlock Formation and Coiling of Meiotic Chromosome Axes During Synapsis

Chung-Ju Rachel Wang, Peter M. Carlton, Inna N. Golubovskaya and W. Zacheus Cande

DOI: 10.1534/genetics.109.108688

FILES S1-S15

Files S1-S15 are available for download as movie files (.mov) at

http://www.genetics.org/cgi/content/full/genetics.109.108688/DC1

File S1: 3D-rotation video of Figure 1A showing the spatial organization of lateral elements, visualized by AFD1 immunostaining, in a whole early pachytene nucleus visualized by 3D-SIM. The bilateral symmetry and twisting of LEs are both visible.

File S2: 3D-rotation video of Figure 1B, showing a more detailed view of the roughly symmetric AFD1 organization.

File S3: 3D-rotation video of Figure 2A, in volume-rendered projection, showing the chromomere organization, centromere and knob structure, and overall nuclear architecture of an early pachytene nucleus stained by DAPI and visualized by 3D-SIM.

File S4: 3D-rotation video of Figure 2B, a chromosome arm stained with DAPI, seen pulling away from the bulk of the nucleus. The movie demonstrates the globular chromomere structure, and the double helical organization of homologs twisting around each other.

File S5: 3D-rotation video of Figure 2D, a chromosome region stained with DAPI and visualized by 3D-SIM, showing chromatin organization of a centromere (dark central region) and its associated pericentric regions (brighter distal regions).

File S6: 3D-rotation video of Figure 2E, showing a heterochromatic knob and the adjacent chromosome arm regions of an early pachytene chromosome, stained with DAPI and visualized by 3D-SIM.

File S7: 3D-rotation video of Figure 2F, showing chromatin organization of the long arm of chromosome 10 in an early pachytene nucleus. The chromosome is stained with DAPI and visualized by 3D-SIM.

File S8: 3D-rotation video of Figure 2G, showing chromatin organization of the long arm of chromosome 10 in a late pachytene nucleus. The chromosome is stained by DAPI and visualized by 3D-SIM.

File S9: 3D-rotation video of Figure 3J showing the lateral elements, detected by AFD1 immunostaining, organized as a left-handed double helix. The handedness is the same along the entire chromosome.

File S10: "Fly-through" video of cross sections of the chromosome shown in Figure 3L, progressing from the left telomere, showing left-handed (counterclockwise) coiling throughout the entire chromosome.

File S11: "Fly-through" video of cross sections of the chromosome shown in Figure 3L, progressing from the right telomere, showing left-handed (counterclockwise) coiling throughout the entire chromosome. Since the slice is moving away from the viewer in both video S10 and S11, the twisting is in the same counterclockwise direction.

File S12: An example of Type I interlock. Two chromosomes whose lateral elements are immunostained with AFD1 are false-colored with green and red; the fully-synapsed red chromosome passes through a synapsis bubble in the green chromosome.

File S13: An example of Type II interlock. Two chromosomes whose lateral elements are immunostained with AFD1 are false-colored with green and red. Each chromosome is synapsed at its ends and contains one interior synapsis bubble; these bubbles interlock with each other.

File S14: An example of a Complex interlock. Four chromosomes are involved and false-colored with green, red, blue and yellow. The green and blue chromosomes are involved in Type I interlocks among each other, while the red chromosome makes Type I interlocks with both green and blue chromosomes, and yellow chromosome makes Type II interlocks with both the red and green chromosomes.

File S15: 3D-rotation video of Figure 5G, showing lateral elements in red (AFD1 immunostaining) and two unsynapsed regions in green (ASY1 immunostaining) which differ in length.

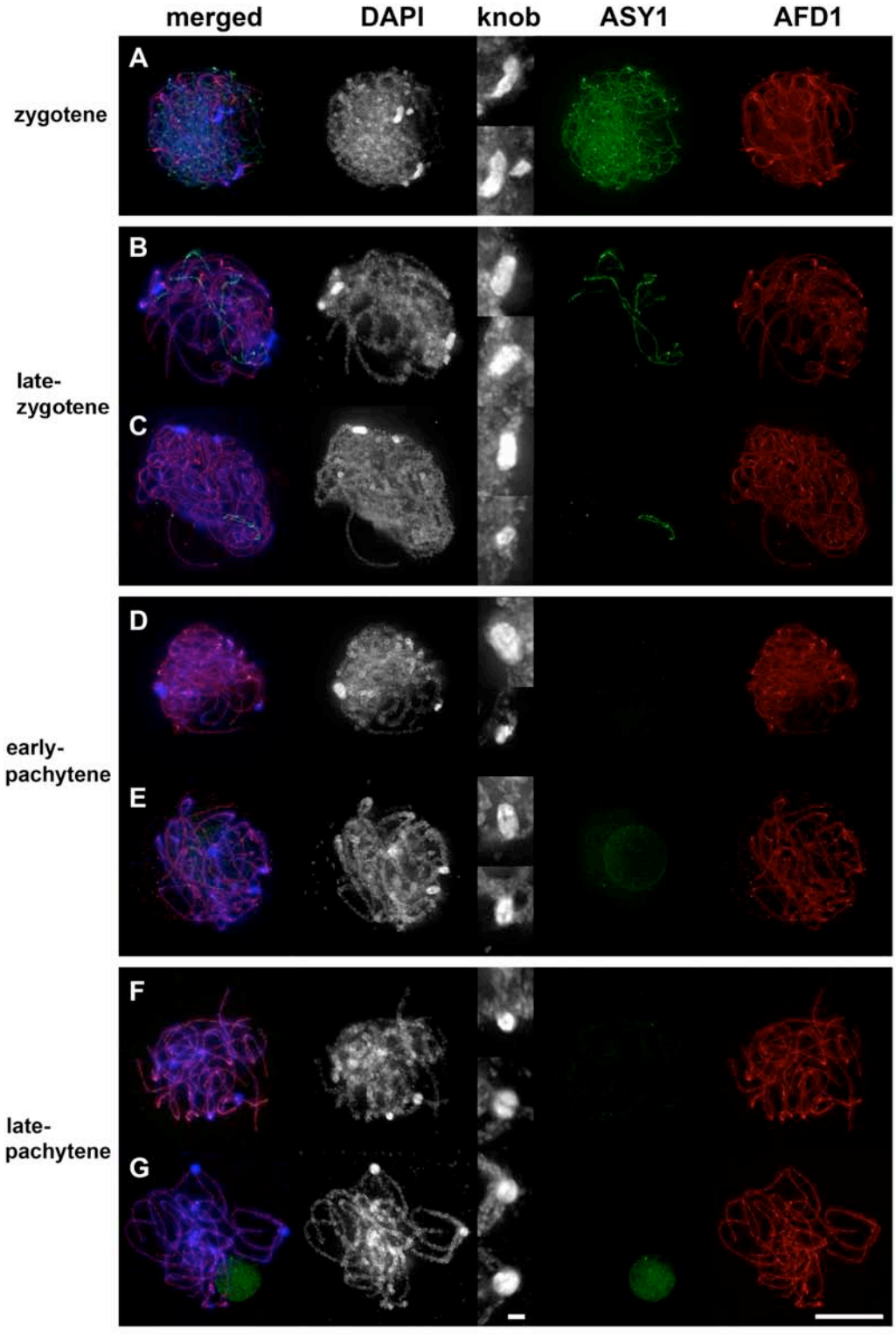

FIGURE S1. — Chromosome morphology changes as criteria for staging and their correlation with extent of synapsis. After the meiotic stages were determined by chromosome morphology, the extent of synapsis was monitored by AFD1 (red) and ASY1 (green) antibody staining pattern. AFD1 antibody stains both unsynapsed and synapsed regions, whereas ASY1 signal is only detected on unsynapsed axes. (A) An example of zygotene nucleus with elongated knobs contains both unsynapsed and synapsed regions. (B-E) Nuclei from a "late zygotene/early pachytene" population have oval shaped knobs. Nuclei in (B and C) were determined as late zygotene because they still contain unsynapsed regions. Nuclei in (D and E) were determined as early pachytene because their synapsis is complete. (F and G) Two nuclei determined as late pachytene because of its spherical knobs exhibit complete synapsis.

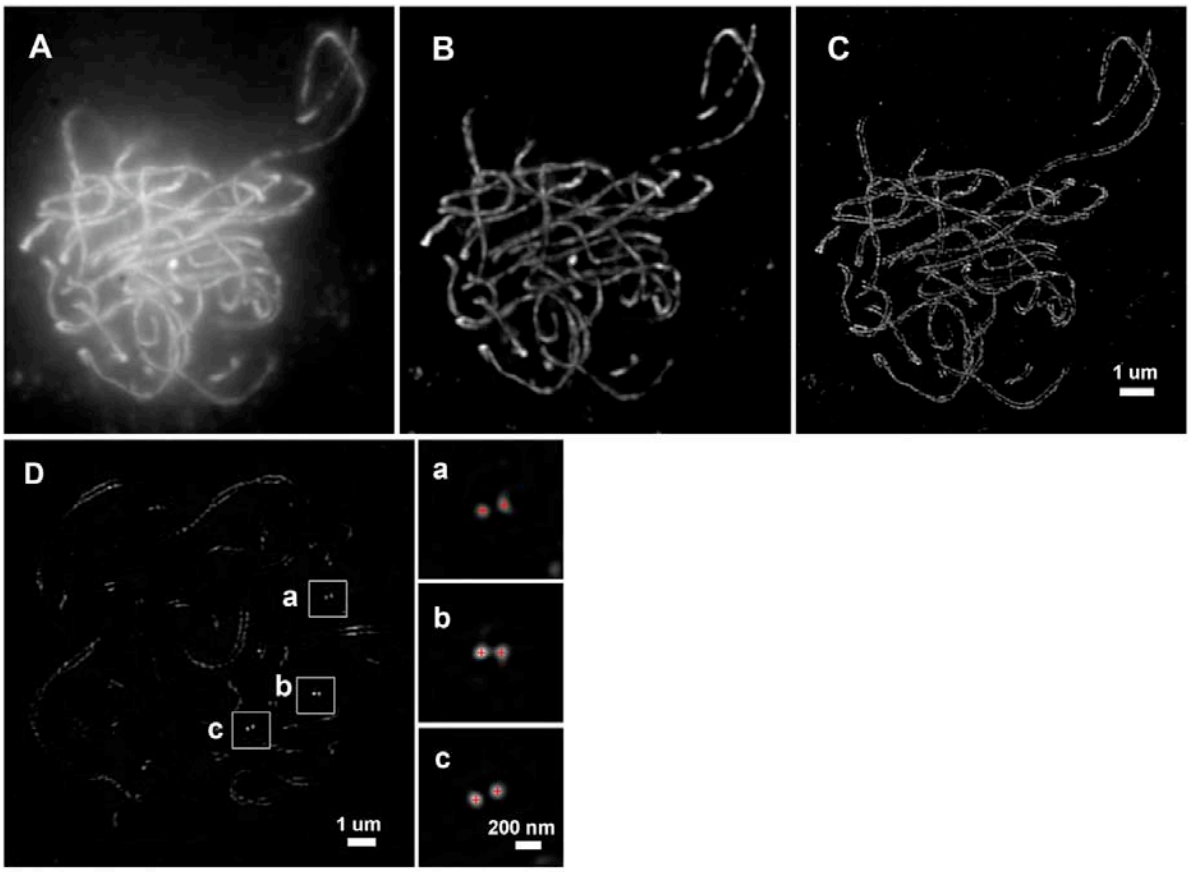

FIGURE S2. — Comparison of lateral element morphology under different microscopy methods. (A) A phase-averaged (equivalent to conventional widefield) partial projection of lateral elements detected with AFD1 immunostaining. (B) The same nucleus after applying constrained iterative deconvolution. (C) The same nucleus under 3D-SIM. The higher resolution of 3D-SIM is demonstrated by the discrimination of both lateral elements in (C) whereas A and B show only single fibers. (D) A cross section of a pachytene nucleus stained with AFD1 antibody. Three insets in (D) as shown in (a), (b) and (c) are three examples for the measurement of the space between AFD1 signals of synaptonemal complex.

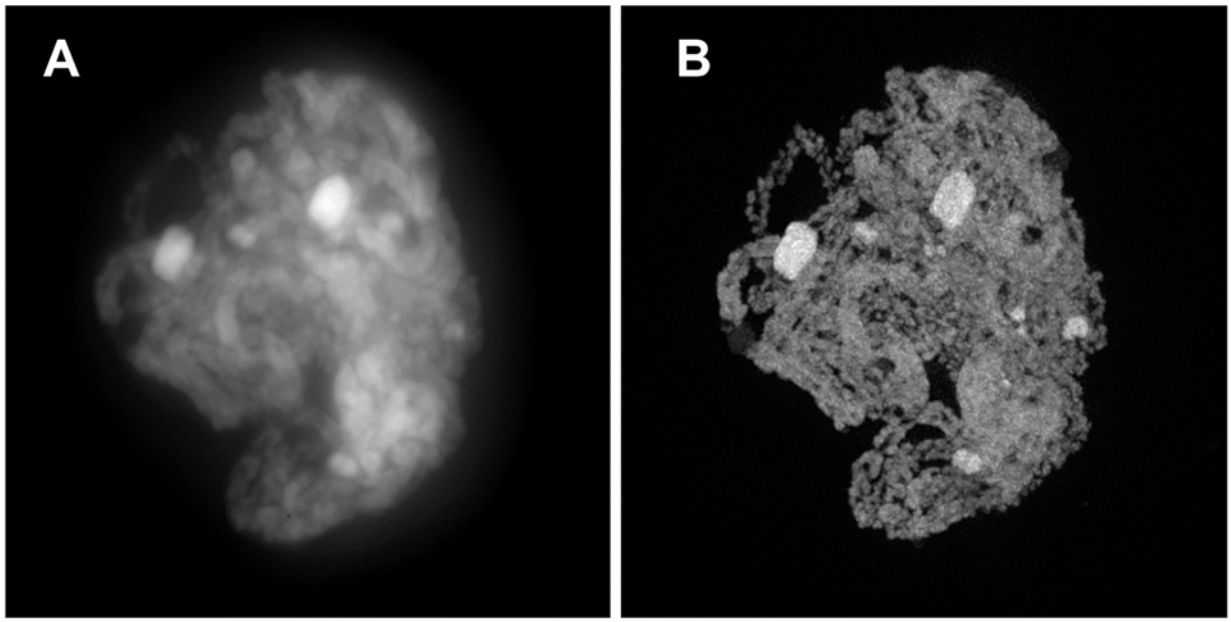

FIGURE S3. — Increased resolution of chromatin structure under 3D-SIM. (A) A full projection of a late zygotene/early pachytene nucleus under conventional fluorescence microscopy. (B) The same nucleus under 3D-SIM. The distinguishing features of B are that homologs can be distinguished, chromomeres are more visible, and substructure of chromomeres can be seen.

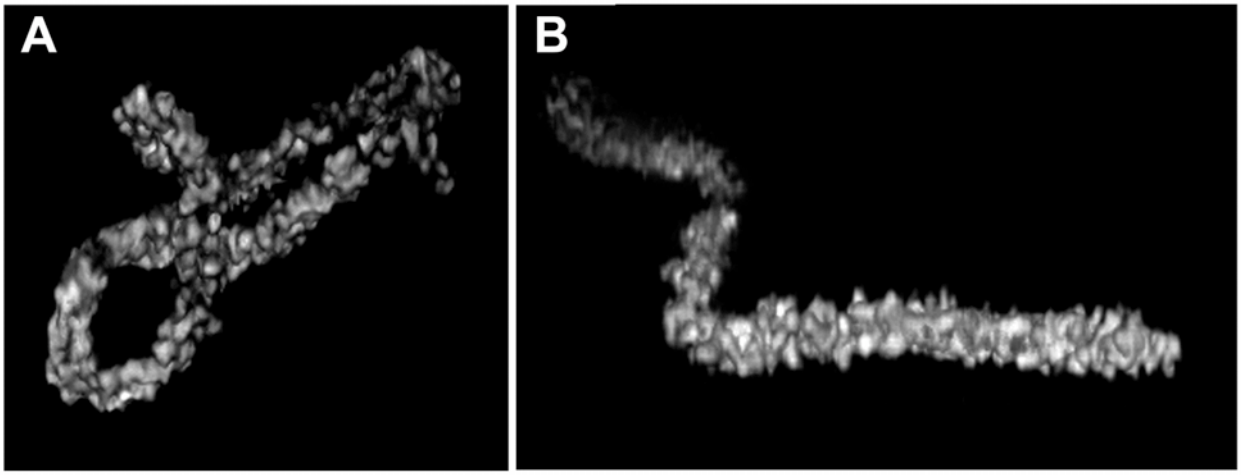

FIGURE S4. — Volume-rendered projections of chromosome 10 at early and late pachytene. A and B show the entire chromosomes whose long arms are depicted in Figures 2F and 2G, respectively. The volume-rendered projection shows the complexity of the surface and strengthens the impression that late pachytene chromosome structure is a result of the compression of early pachytene structure along the chromosome axis.

TABLE S1

Measurement of total chromosome lengths, unsynapsed regions (US), numbers of 180 degree coils and average distance between coils of three late zygotene nuclei and three late pachytene nuclei

Samples	Total length of chromosomes (um)	US/total length	Numbers of 180 degree coils	Distance between coils (um)
late-zygotene cell 1	868	9.1%	242	3.26±1.85
late-zygotene cell 2	689	6.1%	240	2.70±1.18
late-zygotene cell 3	632	2.3%	290	2.13±1.11
Average for late-zygotene nuclei	**729.6**	**5.8%**	**257.3**	**2.66±1.48**
late-pachytene cell 1	434	0%	335	1.29±0.34
late-pachytene cell 2	421	0%	315	1.33±0.45
late-pachytene cell 3	472	0%	340	1.38±0.48
Average for late pachytene nuclei	**442.3**	**0%**	**330**	**1.34±0.43**

TABLE S2

Lengths and ratios of unsynapsed axes

	Lengths of unsynapsed regions (um/um)	Ratio
Unsynapsed regions associated with interlocks	14.7/13.1	1.12
	13.3/10.6	1.25
	7.1/5.5	1.29
	3.9/2.1	1.86
	3.8/2.7	1.41
	4.3/3.8	1.13
	3.3/2.3	1.43
	7.0/6.6	1.06
	5.1/3.1	1.65
	11.6/9.4	1.23
	5.3/2.5	2.12
Average ratio		**1.41±0.33**
Unsynapsed regions not associated with interlocks	7.0/6.7	1.04
	11.1/10.7	1.04
	2.5/2.4	1.04
Average ratio		**1.04±0.003**